Rendiconti
Accademia Nazionale delle Scienze detta dei XL
Memorie e Rendiconti di Chimica, Fisica, Matematica e Scienze Naturali
138° (2020), Vol. I, fasc. 1, pp. 55-60
ISSN 0392-4130 • ISBN 978-88-98075-38-6

The Role of Molecular Orientation in Enantioselective Reactions

FEDERICO PALAZZETTI[1] – ANDREA LOMBARDI[1]
NAYARA DANTAS COUTINHO[2] – MARCOS VINÍCIUS C. S. REZENDE[3]
VALTER-HENRIQUE CARVALHO SILVA[3]

[1] Università degli Studi di Perugia, Dipartimento di Chimica, Biologia e Biotecnologie, 06123, Perugia, Italy.
[2] Instituto de Química, Universidade de Brasília, Brasília, Brazil.
[3] Grupo de Química Teórica e Estrutural de Anápolis, Campus de Ciências Exatas e Tecnológicas, Universidade Estadual de Goiás, Anápolis, Brazil.

* Corresponding author: federico.palazzetti@unipg.it

Abstract – Construction of theoretical models for the characterization of chiral selectivity mechanisms is needed in order to predict and analyze kinetic and dynamic aspects of collisional processes, where chiral molecules are involved. The role played by molecular orientation in chiral discrimination phenomena has been demonstrated by first-principles molecular dynamics simulations for the reaction occurring between the bisulfide anion HS– and oriented prototypical chiral molecules CHFXY (where X = CH_3 or CN and Y = Cl or I). In bimolecular nucleophilic substitution (SN_2), alternative pathways due to the enantiomer forms when molecules are oriented, result in different reactivity of CHFCNI.

Keywords: molecular dynamics simulations; bimolecular nucleophilic substitution; chirality discrimination phenomena

Riassunto – La costruzione di modelli teorici per la caratterizzazione di meccanismi di selezione chirale è necessaria per prevedere e analizzare gli aspetti cinetici e dinamici dei processi collisionali in cui sono coinvolte molecole chirali. Il ruolo svolto dall'orientazione molecolare nei fenomeni di discriminazione chirale viene dimostrato attraverso simulazioni di dinamica molecolare for la reazione tra l'anione bisolufuro HS^- e la molecola chirale prototipo CHFXY (dove X=CH_3 o CN e Y=Cl o I). Nella sostituzione nucleofila bimolecolare (SN_2), percorsi alternativi dovuti alle diverse forme enantiomeriche, per molecole orientate, vengono evidenziati dalla diversa reattività di CHFCNI.

Parole chiave: simulazioni di dinamica molecolare; sostituzione nucleofila bimolecolare; fenomeni di discriminazione della chiralità

Introduction

Molecular alignment and orientation are non-statistical distributions of the rotational angular momentum with respect to a quantization axis [1]. More precisely, molecular alignment consists in the control of the direction of the rotational angular momentum, while molecular orientation concerns not only the control of the direction, but also the sense. Molecular orientation is a fundamental requisite to observe spatial aspects in collision and photodissociation phenomena, that otherwise would be hidden by the molecular random rotation [2]. Assessment of the role of molecular orientation in chirality discrimination processes is a challenge of the OrChiD project [3]. Evidences of the role played by the orientation in chiral discrimination processes have been already demonstrated theoretically for elastic collisions [4]. In that case, elastic collisions between oriented (rigid) hydrogen peroxide (H_2S_2) [5] and hydrogen persulfide (H_2S_2) [6] arguably the simplest chiral molecules, and rare-gas atoms were simulated. The authors could observe that the rare-gas atoms were scattered at different angles, according to the mirror form of the chiral encounter.

We consider two techniques to control the molecular alignment and orientation: (i) the "natural alignment" [7] makes use of a mechanical speed selector, a device that permits to control the translational degrees of freedom of the molecules by selecting the beam velocity and consequently the degree of natural alignment, which occurs in molecular beams, exploiting the "seeding" effect that is the collisions induced by lighter and faster gases, transferring momentum to the molecule and determining the alignment; (ii) the hexapolar orientation technique, which we will focus on this contribution, consists in coupling the aligning electric field of the hexapole, that is, a non-uniform electric field arranged along the propagation axis of the molecular beam, to the orienting electric field of a second element located downstream of the hexapole [8-10].

Experimental and theoretical studies shown that often bimolecular substitution mechanisms, SN_2, occur simultaneously to an alternative competing channel, the bimolecular elimination mechanism, E_2 [11]. These channels are arguably the most fundamental ones in the study of chemical reactions involving organic molecules that permit to establish the stereospecific role for chiral substrates [12].

Several studies had as a subject the determination of the stationary points in minimum energy paths for SN_2 and E_2 channels in the classical gas-phase (see [13, 14] and references therein). The reaction channels involve various mechanisms such as the double inversion indirect one with proton-transfer for the nucleophilic group, that represents one of the most important mechanisms, beside the direct mechanism [15]. Single collision experiments and electronic structure calculations at a high level of theory have been performed to study the competing mechanisms E_2 and SN_2 for the archetypical reaction $X^- + RY$, with X and Y = F, Cl, Br, OH, and CN. Results confirmed that the investigated class of reactions are characterized by the following points: (i) synchronous E_2 transition state, instead of nonconcerted mechanism, with preference for anti-E2 configuration; (ii) change of the leaving halogen atom (from F to I) causes a decrease in the barrier height; (iii) SN_2 with retention of configuration is a lesser favorable pathway and Walden inversion configuration pathway is preferred; (iv) abrupt change from backward to dominant forward scattering depending on the alkyl group in the substrate [16, 17].

In this work, we focus on the role played by the orientation in reactive scattering processes (in the gas phase), namely the Aquilanti mechanism (for further details see Ref. [18]). Molecular dynamics simulations have been performed on the prototypical chiral molecules CHFXY, where X is CH_3 o CN, and Y is Cl or I, reacting with HS^-. From now on, SN_2 and substitution channels will be used as synonyms, as well as E_2 and elimination channels. The article is structured as follows: in Section 2, the methods employed in the work are reported; in Section 3, we give a discussion of the results; final remarks, in Section 4, conclude the paper. (The figures in the article are adapted from Ref. [18]).

Background

Quantum chemical calculations

Optimization of the geometries of reactants, products and transition states, as well as their energies have been calculated at the ωB97XD/ aug-cc-pVDZ level of theory. These latter have been further refined by using coupled cluster method with triple excitations treated perturbatively CCSD(T). For the valence electrons of the iodine atom, the small-core pseudopotential (LANL2DZ) has been employed [19, 20]. The stationary points were characterized by analytic harmonic frequency calculations: the absence or existence of an imaginary frequency indicates that the optimized structures are local minima or transition states, respectively. The zero-point vibrational energy contributions have been considered in

the calculation of the energy barriers. Calculations have been performed by the Gaussian09 package [21].

Reaction rate

The deformed-transition state theory [22], implemented in the Transitivity code [23] (www.vhcsgroup.com/transitivity), has been employed to calculate the reaction rate constants as a function of the temperature $k(T)$. For a general bimolecular reaction, the rate constant is given by:

$$k(T) = \frac{k_B T}{h} \frac{Q^{\neq}}{Q_1 Q_2} \left(1 - d \frac{\varepsilon^{\neq}}{k_B T}\right)^{1/d} \quad (1)$$

where k_B is the constant of Boltzmann ($1.38 \cdot 10^{-23}$ J·mol^{-1}); h is the constant of Planck ($6.63 \cdot 10^{-34}$ J·s); Q_1, Q_2 and $Q^{\neq}$ are the partition functions of the reactant 1, 2 and transition complex, respectively; $\varepsilon^{\neq}$ is the effective height of the energy barrier that is given by the sum of the harmonic zero-point energy correction and the height of the potential energy barrier; finally, d is given by the equation

$$d = -\frac{1}{3}\left(\frac{h\nu^{\neq}}{2\varepsilon^{\neq}}\right)^2 \quad (2)$$

where $\nu^{\neq}$ is the penetration frequency for crossing the barrier.

For practical purposes, an alternative to the Arrhenius equation fitting is obtained by formulating the Aquilanti-Mundim equation [24, 25]

$$k(T) = A\left(1 - \bar{d}\frac{E_0}{k_B T}\right)^{1/\bar{d}} \quad (3)$$

where A and $\bar{d}$ are the pre-exponential factor and the deformation parameter, respectively. (Note a change in the notation here, needed to avoid ambiguities: in terms of the fitted equation, we defined $\bar{d}$ which is slightly different from d and E_0 which is slightly different from $\varepsilon^{\neq}$.)

Molecular Dynamics Trajectories

First-principle Born-Oppenheimer molecular dynamics simulations have been performed by the CPMD 3.17.1 package [26]. The system has been modeled using a periodically repeated cubic cell of side-length 13 Å, containing one HS– and one CHFCNI (chiral) molecule. Simulations have been performed for the two enantiomeric forms R and S, starting from the same initial reciprocal position of HS- with respect to CHFCNI. The electronic structure has been treated within the generalized gradient approximation to density functional theory, using the Perdew– Burke–Ernzerhof (PBE) exchange-correlation functional [27]. Vanderbilt ultrasoft pseudopotentials have been employed to represent core-valence electron interactions [28]. A planewave basis set has been used to expand the valence electronic wave functions with an energy cutoff of 25 Ry. The equations of motion have been integrated using a time step of 5 a. u. (0.121 fs) for a total time of 1.8 ps. The simulations have been conducted in an NVT ensemble at temperature of 200 K controlled using a Nosé-Hoover thermostat [29].

Results and Discussions

In Fig. 1, the transition state structures of the six reactions studied, both for R and S enantiomers, at the ωB97XD/aug-cc-pVDZ level of theory are reported. The reaction channels we have considered, the anti-E_2, [(1) and (2) reactions], and back-side SN_2, [(3) to (6) reactions], are the most energetically favored. The transi-

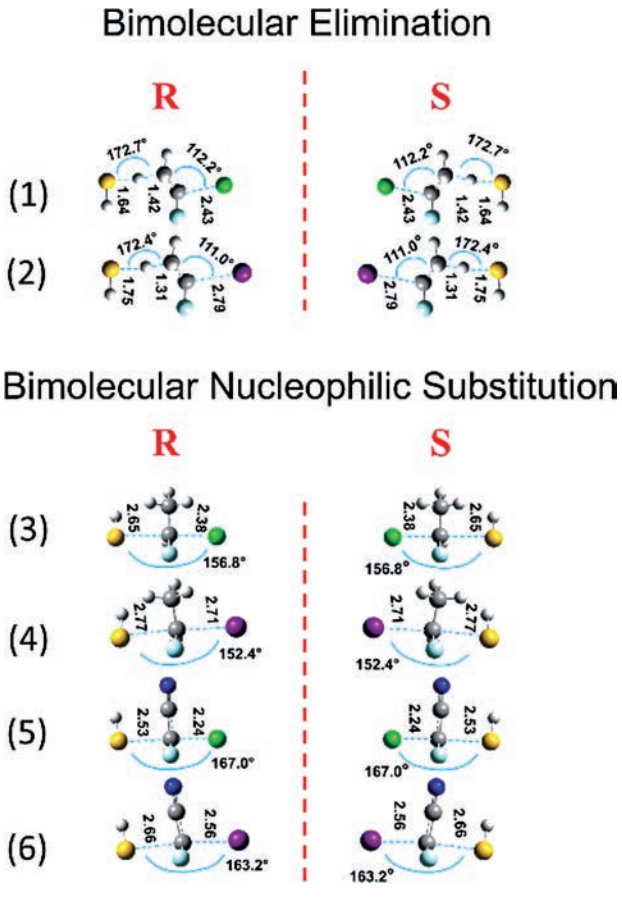

Fig. 1. Transition state structures of the six examined reaction channels. Obviously, the six enantiomer pairs R and S present identical bond lengths and angles.

tion state structures of both elimination and substitution channels present similarities, except for the C–Y bond length. Also, in the SN_2 channels, there is a variation of about 10° in the S – $\hat{C}$ – Y angle, depending on the CN and CH_3 group connected to the central carbon. (For further details, see Ref. [18]). Thermodynamics and kinetics parameters with zero-point energy have been calculated at the CCSD(T)/aug-cc-pVDZ//ωB97XD/aug-cc- pVDZ level of theory and are reported in detail in Ref. 18. Here, we report the most significant properties, useful for the discussion of the results. The substitution channels SN_2 are exothermic; the elimination channels E_2 (Cl as leaving group) are thermoneutral (1) and endothermic (2). The spontaneity of the reactions has been evaluated by calculating the Gibbs-free energy change ΔG: all the reactions are characterized by ΔG<0, while reaction (2), for both R and S configurations, are the only characterized by ΔG>0. The elimination channels present the highest barrier height, 10 kcal/mol for the elimination of Cl and 13 kcal/mol for the elimination of the I atom. For the substitution channels the barrier heights are lower, *ca.* 5 kcal/mol. The d-TST formulation has been employed to obtain the rate constants for the HS^-+ $CHFCH_3Y$ (Y=Cl or I) reactions in a wide range of temperature (200–4000 K) at CCSD(T)/aug-cc-pVDZ//ωB97XD/ aug-cc-pVDZ level of calculation. The rate constants are expressed by the Aquilanti-Mundim formula:

$$CHFCH_3Cl\ (SN_2)\ k = 6.29\cdot10^{14}\ cm^3mol^{-1}s^{-1}\ (1+724.21/T)^{-10.13} \quad (4)$$

$$CHFCH_3I\ (SN_2)\ k = 6{:}61\cdot10^{14}\ cm^3mol^{-1}s^{-1}\ (1+528.45/T)^{-14.14} \quad (5)$$

$$CHFCH_3Cl\ (E_2)\ k = 1{:}65\cdot10^{16}\ cm^3mol^{-1}s^{-1}\ (1+363.92/T)^{-34.97} \quad (6)$$

$$CHFCH_3I\ (E_2)\ k = 7.09\cdot10^{15}\ cm^3mol^{-1}s^{-1}\ (1+288{:}03/T)^{-45.98} \quad (7)$$

and are employed to calculate the branching ratios through the equation

$$\frac{k_{SN_2}}{k_{SN_2}+k_{E_2}} \quad (8)$$

or

$$\frac{k_{E_2}}{k_{SN_2}+k_{E_2}} \quad (9)$$

In Figure 2, we report the branching ratio between the elimination and substitution channels for the reaction $CHFCH_3Cl+HS^-$ having as products $HSCHFCH_3+Cl^-$ for SN_2 and $CHFCH_2 + H_2S + Cl^-$ and for the reaction $CHFCH_3I+HS^-$ with $HSCHFCH_3+I^-$ as a product of the substitution channel and $CHFCH_2$ + H_2S + Cl^- as a product of the elimination channel. The SN_2 channel is the preferred one at low temperatures.

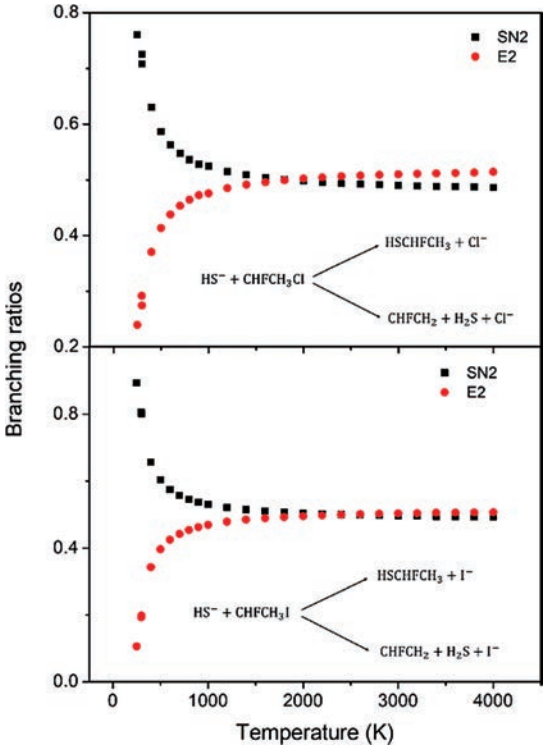

Fig. 2. Branching ratios of the competing channels SN_2 and E_2. (Upper panel) The reactions HS^- + $CHFCH_3Cl \rightarrow HSCHFCH_3$ + Cl^- (SN_2 channel) and HS^- + $CHFCH_3Cl \rightarrow CHFCH_2$ + H_2S + Cl^- (E_2 channel). (Lower panel) The reactions HS^- + $CHFCH_3I \rightarrow$ $HSCHFCH_3$ + I^- (SN_2 channel) and HS^- + $CHFCH_3I \rightarrow CHFCH_2$ + H_2S + I^- (E_2 channel).

As the temperature increases the E2 channel becomes more important until reaching 0.5 at temperatures higher than 1500 K.

In Figure 3, we report the energy profile of the reaction CHFCNI + HS^-. The reaction path is characterized by a "submersed" barrier at 1.8 kcal/mol under the energy of the reactants. This is the typical case of those reactions that exhibit negative dependence on the rates. The entrance and exit complexes are also reported, with energies with respect to the reactants of -21.7 and -29.8 kcal/mol, respectively. Reactive trajectories have been monitored by following the coordinate *s*, defined as the difference between the length of the breaking bond (r_1 = C–I) and the length of the forming bond (r_2 = C–S). In Figure 4, *s* is reported as a function of time for the substitution channels of the reaction CHFCNI + HS^- for both the enantiomers R and S. The plot shows a different reactivity between the R and S enantiomers, denoted by the different dependence of *s* on the time. More precisely, R is characterized by a lower reactivity, requiring longer reaction time. These simulations confirm that the

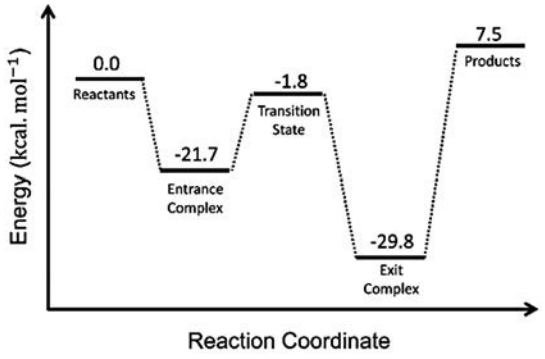

Fig. 3. The energy profile in kcal/mol of the reaction HS^- + CHFCNI → HSCHFCNI + I^-.

orientation is a fundamental requisite in enantioselective mechanisms, the so-called Aquilanti mechanism.

Final Remarks

Thermodynamic and kinetic properties of CHFXY (X = CH_3 or CN and Y = Cl or I) + HS^- reactions, evolving through elimination, E_2, and substitution, SN_2, channels, have been investigated by stationary electronic structure methods and Born-Oppenheimer first-principle molecular dynamics simulations spanning a wide range of temperatures. The Aquilanti mechanism, *i. e.* the role played by molecular orientation in enantioselective reactions has been demonstrated for the reaction CHFCNI + HS^- → HSCHFCN + I^-, by evidencing a different reactivity between the two oriented enantiomers.

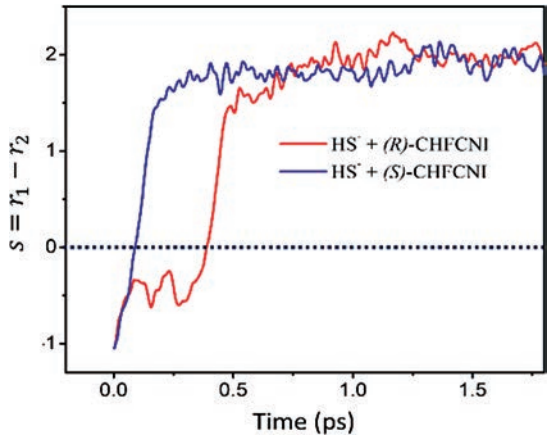

Fig. 4. The evolution in time of the difference between the bond length of the breaking bond C – F and the forming bond C – S, namely $s = r_1 - r_2$, for the reaction HS^- + CHFCNI involving both enantiomers R and S.

Further developments of models of chiral discrimination processes are conditioned by the limits due to the accuracy of the quantum mechanics methods employed. The state-of-the-art of these methods for the determination of small energy differences between different quantum states, the evaluation of intermolecular forces and calculations involving different electronic states, is still far to yield results enough accurate to permit univocal interpretations and predictions of the experiments, especially for what concerns photoinitiated processes, characterized by the involvement of a dense manifold of electronic states. This limit can be reversed, and the experiment becomes fundamental to calibrate ad evaluate the accuracy of calculations, especially those based on the density functional theory.

Acknowledgement

The authors gratefully acknowledge the Italian Ministry for Education, University and Research, MIUR, for financial support: SIR 2014 "Scientific Independence of young Researchers" (RBSI14U3VF). The authors are grateful for the support given by Brazilian CAPES and CNPq and by High-Performance Computing Center at the Universidade Estadual de Goiás (UEG). Valter H. Carvalho-Silva thanks CNPq for the research funding programs [Universal 01/2016 - Faixa A - 406063/2016-8]. The authors acknowledge Vincenzo Aquilanti for the fruitful discussions.

BIBLIOGRAPHY

[1] Aquilanti, V., Bartolomei, M., Pirani, F. *et al.*: Orienting and aligning molecules for stereochemistry and photodynamics. *Phys. Chem. Chem. Phys.* 7, 291-300 (2005). https://doi.org/10.1039/b415212c

[2] Aquilanti, V., Maciel, G. S.: Observed molecular alignment in gaseous streams and possible chiral effects in vortices and in surface scattering. *Orig. Life Evol. Biosph.* 36, 435-441 (2006). https://doi.org/10. 1007/s11084-006-9048-z

[3] Aquilanti, V., Casavecchia, P., Che, D. -C., Falcinelli, S., Lin, K. -C., Lombardi, A., Kasai, T., Nakamura, M., Palazzetti, F., Pirani, F., Tsai, P. -Y.: The ORCHID project: a search for the Origin of Chiral Discrimination. Rendiconti Accademia Nazionale delle Scienze detta dei XL Memorie di Scienze Fisiche e Naturali 136° (2018), Vol. XLII, Parte II, Tomo II, pp. 163-173.

[4] Aquilanti, V., Ascenzi, D., Cappelletti, D., Pirani, F.: Velocity dependence of collisional alignment of oxygen molecules in gaseous expansions. *Nature* 371, 399-402 (1994). https://doi.org/10.1038/ 371399a0

[5] Lombardi, A., Palazzetti, F., Maciel, G. S. *et al.*: Simulation of oriented collision dynamics of simple chiral molecules. *Int. J. Quant. Chem.* 111:1651 (2011).

[6] Barreto, P. R. P., Vilela. A. F. A. Lombardi A, *et al.*: The hydrogen peroxide-rare gas systems: quantum chemical calculations and hyperspherical harmonic representation of the potential energy surface for atom-floppy molecule interactions. *J. Phys. Chem. A* 111:12754-12762 (2007). https://doi.org/10.1021/jp076268v

[7] Maciel, G. S., Barreto, P. R. P., Palazzetti, F. *et al.*: A quantum chemical study of H_2S_2: intramolecular torsional mode and intermolecular interactions with rare gases. *J. Chem. Phys.* 129: 164302 (2008). https:// doi.org/10.1063/1.2994732

[8] Che, D.-C., Palazzetti, F., Okuno, Y., Aquilanti, V., Kasai, T.: Electrostatic hexapole state-selection of the asymmetric-top molecule propylene oxide. J. Phys. Chem. A 114, 3280-3286 (2010).

[9] Che, D.-C., Kanda, K., Palazzetti, F., Aquilanti, V., Kasai, T.: Electrostatic Hexapole State-Selection of the Asymmetric-Top Molecule Propylene Oxide: Rotational and Orientational Distributions. Chem. Phys. 399, 180-192 (2012)

[10] Palazzetti, F., Maciel, G. S., Kanda, K., Nakamura, M., Che, D.-C., Kasai, T., Aquilanti, V.: Control of conformers combining cooling by supersonic expansion of seeded molecular beams with hexapole selection and alignment: experiment and theory on 2-butanol. Phys. Chem. Chem. Phys. 16, 9866-9875 (2014).

[11] Carrascosa, E., Meyer, J., Zhang, J. *et al.*: Imaging dynamic fingerprints of competing E_2 and SN_2 reactions. *Nat. Commun.* 8, 25 (2017). https://doi.org/10.1038/s41467-017-00065-x

[12] Smith, M. (2013) March's advanced organic chemistry: reactions, mechanisms, and structure., 7th Edition. Wiley.

[13] Hamlin, T. A., Swart M., Bickelhaupt, F. M.: Nucleophilic substitution (SN_2): dependence on nucleophile, leaving group, central atom, substituents, and solvent. *Chem. Phys. Chem.* 19, 1315-1330 (2018). https://doi.org/10.1002/cphc.201701363

[14] Piccini, G., McCarty, J., Valsson, O., Parrinell, M.: Variational flooding study of a SN_2 reaction. *J. Phys. Chem. A* 8, 580-583 (2018). https://doi.org/10.1021/jp900576x

[15] Szabó, I., Czakó, G.: Revealing a double-inversion mechanism for the F[−] + CH_3Cl SN_2 reaction. *Nat. Commun.* 6: 5972 (2015). https://doi.org/10.1038/ncomms 6972

[16] Ma, Y.-T., Ma, X., Li. A. *et al.*: Potential energy surface stationary points and dynamics of the F^-+CH_3I double inversion mechanism. *Phys. Chem. Chem. Phys.* 19, 20127-20136 (2017). https://doi.org/10.1039/ C7CP02998E

[17] Carrascosa, E., Meyer, J., Michaelsen, T. *et al.* Conservation of direct dynamics in sterically hindered SN_2/E_2 reactions. Chem Sci 9:693-701 (2018). https://doi.org/10.1039/C7SC04415A

[18] Rezende, M. V. C. S., Coutinho, N. D., Palazzetti, F., Lombardi, A., Carvalho-Silva, V. H.: Nucleophilic substitution vs elimination reaction of bisulfide ions with substituted methanes: exploration of chiral selectivity by stereodirectional first-principles dynamics and transition state theory. *J. Mol. Mod.* 25, 227 (2019).

[19] Yang, L., Zhang, J., Xie, J. *et al.*: Competing E_2 and SN_2 mechanisms for the F^- + CH_3CH_2I reaction. *J. Phys. Chem. A* 121, 1078-1085 (2017). https://doi.org/10.1021/acs.jpca.6b09546

[20] Xie, J., Ma, X., Zhang, J. *et al.*: Effect of microsolvation on the OH^- $(H_2O)_n$ + CH_3I rate constant. Comparison of experiment and calculations for OH^- $(H_2O)_2$ + CH_2I. *Int. J. Mass. Spectrom.* 418: 122-129 (2017). https://doi.org/10.1016/J.IJMS.2016.10.017

[21] Frisch, M. J., Trucks, G. W., Schlegel, H. B., *et al.*: Gaussian 09 Revision E.01

[22] Carvalho-Silva, V. H., Aquilanti, V., de Oliveira, H. C. B., Mundim, K. C.: Deformed transition-state theory: deviation from Arrhenius behavior and application to bimolecular hydrogen transfer reaction rates in the tunneling regime. *J. Comput. Chem.* 38:178-188 (2017). https:// doi.org/10.1002/jcc.24529

[23] Machado, H. G., Sanches-Neto, F. O., Coutinho, N. D., Mundim, K. C., Palazzetti, F., Carvalho-Silva, V. -H. "Transitivity": A Code for Computing Kinetic and Related Parameters in Chemical Transformations and Transport Phenomena. *Molecules*, 24, 3478 (2019).

[24] Sanches-Neto, F. O., Coutinho, N. D., Silva, V.: A novel assessment of the role of the methyl radical and water formation channel in the CH_3OH + H reaction. *Phys. Chem. Chem. Phys.* 19, 24467-24477 (2017). https://doi.org/10.1039/C7CP03806B

[25] Aquilanti, V., Mundim, K. C., Elango, M. *et al.*: Temperature dependence of chemical and biophysical rate processes: phenomenological approach to deviations from Arrhenius law. *Chem. Phys. Lett.* 498, 209-213 (2010). https://doi.org/10.1016/j.cplett.2010.08.035

[26] CPMD version 4.1, CPMD version 3.17.1 (2012) Copyright IBM

[27] Perdew, J. P., Burke, K., Ernzerhof, M.: Generalized gradient approximation made simple. *Phys Rev Lett.* 78:1396 (1997).

[28] Vanderbilt, D.: Soft self-consistent pseudopotentials in a generalized eigenvalue formalism. *Phys Rev B* 41, 7892-7895 (1990). https:// doi.org/10.1111/bdi.12080

[29] Martyna, G. J., Klein, M. L., Tuckerman, M.: Nose–Hoover chains: the canonical ensemble via continuous dynamics. *J. Chem. Phys.* 97, 2635-2643 (1992). https://doi.org/10.1063/1.463940